Modeling and Construction of a Two-Axis Sun Tracking System for a Mobile Solar Cell Panel

Khalid Elias Hammo, Dr. Zakariya Yahya Mohammad

Abstract— In this work, a mobile sun tracking system has been investigated both, theoretically and experimentally. The system deals with direct sun beams while it is attached to a moving vehicle. The system is designed to rotate in azimuth and altitude directions, using two permanent magnate D.C motors. Altitude and azimuth rotational disturbances are produced by the profile of the road on which the vehicle is driven. The theoretical part is focused on the dynamical analysis of the panel rotation using Lagranges formulation and examining the system performance by simulation using SIMULINK. Simulation and experimental tests were performed for azimuth tracking, altitude tracking and the combination of the both while the system is in motion. In each test, it continuously tracks the sun in a reasonable manner, showing the same trends of performance, giving a transient error difference of about (4.50), in maximum, during tracking to end, with almost zero error in the tracking. For a particular test, with short duration and multiple turns of the vehicle, the net collected energy by the mobile sun tracking system is greater than that without tracking. It gives a tracking effectiveness of about (27%) more.

Index Terms— Two axes tracking system, mobile solar cell, dynamic modeling of tracking system.

NOMENCLATURE

K_R	Rotational Kinetic energy	R_1	The normal distance between the panel and rotating axis.
K_T	Translational Kinetic energy	R	Normal distance between the counter balancing mass and rotating shaft axis.
I_e	Reduction gear equivalent moment of inertia	E_{PF}	Collected energy without tracking.
θ	Azimuth angle.	E_C	Consumed energy by motors.
β	Altitude angle.	$I_{alt-sh.}$	the moment of inertia of the rotating shaft in altitude direction.
β_{abs}	Instantaneous absolute angular error in altitude rotation.	$m_{alt-sh.}$	the mass of the rotating shaft in altitude direction.
$\theta_{abs.}$	Instantaneous absolute angular error in azimuth rotation..	$r_{sh.}$	the radius of the rotating shaft in altitude direction.
α	Angle of the sun with vertical	m_b	The counter balancing mass
T_{az}	Motor torque in azimuth tracking.	r_b	Radius of the cylinderical counter balancing mass
T_{alt}	Motor torque in altitude tracking.	$I_{az-sh.}$	the moment of inertia of the rotating shaft in azimuth direction.
ω_{az} or $\dot{\theta}$	Angular speed in azimuth tracking.	$m_{az-sh.}$	the mass of the rotating shaft in azimuth direction.
ω_{alt} or $\dot{\beta}$	Angular speed in altitude tracking.	m_{pv}	Mass of the panel

1 Introduction

Humans are becoming more conscious of environmental protection seeking new energy sources that cause less pollution and do not threaten the environment. For this reason, utilization of solar energy becomes more and more important. The photovoltaic conversion attracts the contemporary researchers to optimize this technique because solar energy is clean, renewable and abundant in every part of our world. [1].

There are two types of systems which utilize solar energy on large scale. The first one is the concentrating type and the other without concentration. The flat plate or photovoltaic panels belong to the latter type, whereas the parabolic mirrors belong to the former. In either of the two cases, one can enhance the efficiency of the system by tracking. [2]. A number of investigations have been performed to design and employ immobile solar tracking systems, such as, closed loop technique with PID controller or using Maximum Power Point Tracking. Abu Haneih A. et al [3], designed and constructed a two degree of freedom orientation system for the photovoltaic panels. They used the closed-loop control to track the sun, when the sky is shiny with no clouds. Figueiredo J. M. et al [4] their study, have focused on the optimization of the electric energy produced by photovoltaic solar cell panels through the development of a passive sun tracking system using a programmable logic controller (PLC). Mamlook R. [5], constructed a two-axis sun tracking system utilizing a (PLC). He compared the results of a tracking system with those obtained from a fixed panel system. Tegeder T. [6], designed and constructed a solar powered Unmanned Aerial Vehicle ((UAV)) capable of tracking the sun for maximum solar energy which is captured via a single axis solar tracking system. Visa I., et al [7], build a sun tracking system that operates in two-axes as a multi-body system. It is defined as a collection of bodies with large translational and rotational movements linked by simple or composite joints. Pratik Pawar, et al [8], designed and constructed a dual axis solar tracking system using Arduino. The system is designed to resist weather, temperature and minor mechanical stress. Tomas de J. M. J. et al, [9], have presented a smart system for energy management using a solar tracking mechanism for a mobile PV panels on an unmanned vehicle devoted to exploration tasks. Details of the work is focused on the batteries storage and charging networks. K. Bhas Kar, et al, [10] developed a GSM communication network for controlling a vehicle. The power of the driving motor is supplied from a rechargeable battery attached to the tracking system. The work is concentrated on the communication with the vehicle by the GSM network. A different issue, but it is related to the aim of this work, Mars rover twin spirit and opportunity were launched and landed in 2004. They became silent and inactive on March 2010 and June 2018 respectively [11]. This was attributed to the lack of energy conversion due to the deposition of dust on the horizontally fixed PV panels. The insufficient collected energy reduces more and more over time. When opportunity was on North-facing slops of Mar, a substantial increase of the solar arrays power output was obtained, as they were tilted towards the Sun, [12]. It is believed that, if the supporting frame of the PV panels were designed to track the sun arrays, continuously, more energy should have been absorbed to charge the batteries. Another benefit, is less amount of Mars dust accumulates on the PV panels, due to their angular mobility during the Sun tracking. These should increase the activity period of such a mobile robot. It is noticed that non of these investigations went through the detailed dynamic analysis of the photo-voltaic panel during rotation, and when it is attached to a moving frame such as land or water vehicles. In this work, the effect of mobility of the panel is investigated both, theoretically and experimentally as it rotates on two axes (azimuth and altitude), while it is attached to a moving land vehicle or car. The theoretical study is focused on the dynamic analysis of the rotating panel and developing the mathematical model of the whole mobile tracking system. Simulation of the system has been performed to show the system behavior, so that, a comparison can be made with that obtained from the experimental set up. The hardware part of the work includes the mechanical design, construction of the system and building a suitable sensors, amplifier and control circuits.

2 System Description

A sun tracking system is considered as mechatronics device. It consists of two subsystems. The first contains the mechanical structure holding the PV panel including the panel it's self as a mass or a body. All parts are given in appendix A with their mass moment of inertia. The second comprises the sensors, the electronic and the electric parts, which includes the controller, the comparator circuit and the power amplifier. The driving D.C. motors are suitably connected to the rotating body via reduction gear and to be supplied by the required power from a (6 volt) rechargeable battery. For torque measurements, a 1-ohm resistance has been added serially to the armature resistance so that the voltage drops which is equivalent to the current can be recorded for determining the total motor's torque using the motor torque constant. Figures (1) and (2) show the tracking system as a two axes rotational system. A photograph of the system on the vehicle is shown in figure (1c).

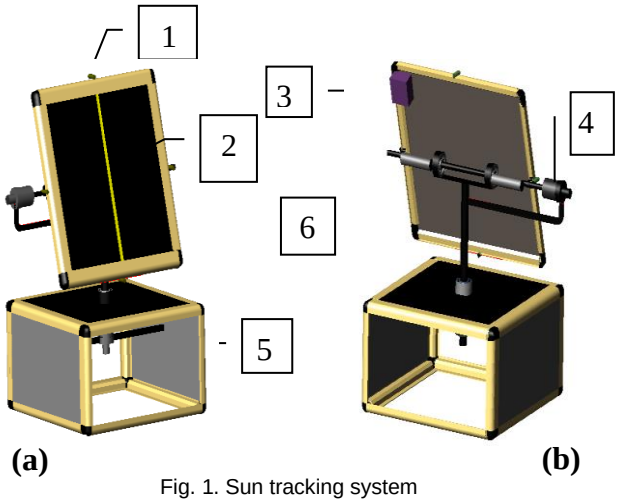

Fig. 1. Sun tracking system
(a) (front view)
(b) (back side view)
(c) photograph of the

1. Optical sensor.
2. PV Panel.
3. Counter Masses.
4. D.C. motor for altitude rotation.
5. D.C. motor for azimuth rotation.
6. Fixing frame.

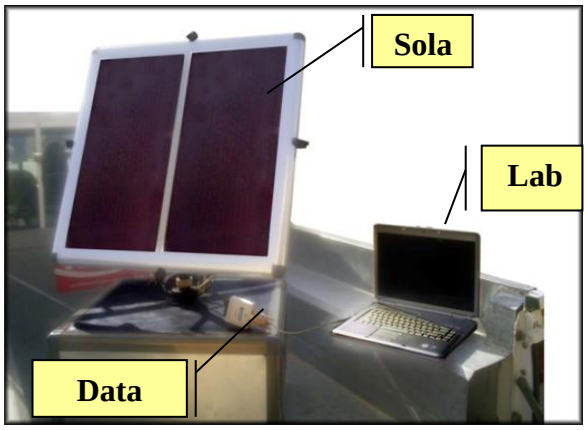

The tracking scheme, in principal, is based on obtaining a differential signal between the two-opposite identical, with 450 inclination, optical sensors that attached at the panel edges. This principal is applied on azimuth and altitude tracking independently, whence the difference between the two signals is zero, the motor current, hence the torque, becomes zero too. This should indicate that the sun rays are normal to the photovoltaic panel. Thus, the system would respond only to angular disturbances and to the initial angular position in the search mode in simulation and experimental tests. The motor stands as a breaking element to prevent the panel rotation due to wind forces. Details about the driving motor arrangements, the electronic circuits, the optical sensors used and their calibration procedure, together with the results of some pliminary experiments may be found in ref. [13].

3 Modeling and Construction of the System

In order to proceed in explaining the system, it is necessary to start with dynamic analysis. It is found useful to use Lagrangian dynamical technique in understanding the system dynamics and developing the system's mathematical model. Figure (2-a), illustrates the case of the panel rotation in azimuth only and the case of simultaneous two axes rotation of the system where motion variables are as shown, figure (2-b).

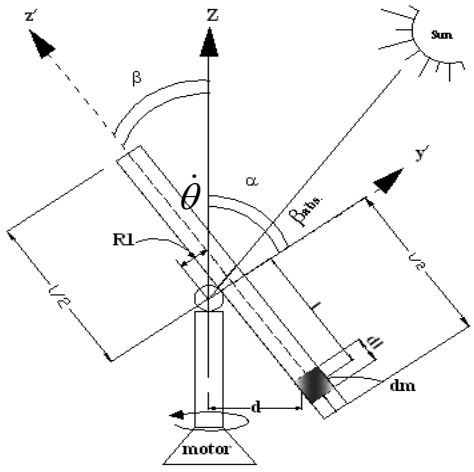

Fig. 2. a)) The rotation of th panel in azimuth direction.

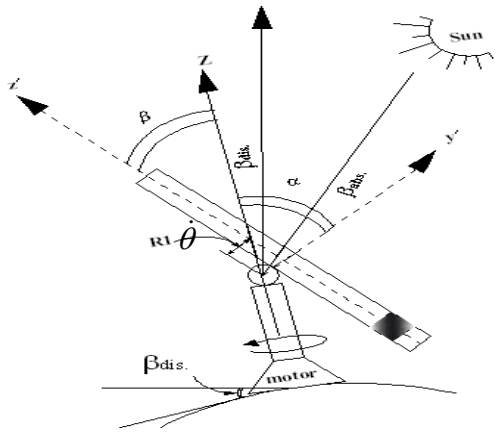

Fig. 2. b)) The rotation of panel in azimuth direction with a disturbance in altitude.

3.1 Lagrangian Equation of motion

The use of Lagrange's equation requires the utilization of two important concepts. These are the kinetic and potential energies. The Lagrangians is defined as the difference between the kinetic energy (K) and the potential energy (U) of the system [14]

$$L(q,\dot{q}) = K(q,\dot{q}) - U(q) \qquad (1)$$

Where: (q) and ($\dot{q}$) are the position and velocity of the components respectively.
the Lagrange's equation is given by:

$$\frac{d}{dt}\left[\frac{\partial L(q.\dot{q})}{\partial \dot{q}}\right] - \frac{\partial L(q,\dot{q})}{\partial q} = T \qquad (2)$$

Where T denotes the force or torque producing the motion.
The translational part in this analysis would give the forces required for fixing the system on the carrier frame to give the translational motion (i.e. have not influenced the rotation of the solar cell panel).
the translational total kinetic energy (K_T) of a body is:

$$K_T = \frac{1}{2}Mv^2 = \frac{1}{2}M(\dot{s})^2 = \frac{1}{2}M\left(\dot{x}^2 + \dot{y}^2 + \dot{z}^2\right) \qquad (3)$$

Here, $v = \dot{s}$, is the magnitude of the velocity vector ds/dt, having components in x, y and z directions. In translational motion, the potential energy is:

$$U = Mgz \qquad (4)$$

The forces in x, y and z directions can be determined using equations (1) to (4) to obtain: Fx = Max , Fy = May and Fz = M (az + g).

Where: ax , ay and az are the translational acceleration components. M is the total mass of the system

The above-mentioned forces represent the reaction forces required to fix the tracking system to the vehicle with no rotation. Naturally, additional torques are transmitted to the base during tracking. The kinetic energies of all rotating parts must be considered. These rotating parts are the solar cell panel, balancing masses, rotating shafts….., etc. Equation (2) may be utilized to determine (T_{az}) and (T_{alt}) which represent the torques for the azimuth and altitude rotation respectively. The rotational kinetic energy (K_R) of a rotating part is given by:

Kinetic energy (K_R) = 0.5 (mass moment of inertia x angular velocity squared). To facilitate the determination of the required motors torque, altitude and azimuth rotations are considered. The overall kinetic energy in altitude rotation is:

$$K.E. = \frac{1}{2}\dot{\beta}_{abs.}^{\,2}\left[\begin{array}{l}\left(\frac{1}{12}m_{pv}\left(l^2+t^2\right)+m_{pv}R_1^{\,2}\right)+2\left[\frac{1}{2}m_b r_b^{\,2}+m_b\times R^2\right]\\+m_{alt-sh.}\times r^2{}_{sh.}+I_e\end{array}\right] \quad (5)$$

Where: $(\dot{\beta}_{abs.})$ is the angular velocity of the panel in altitude.

$(l\ ,t\ )$ are the length and thickness of the panel.

In azimuth rotation, the value of the mass moment of inertia of the rotating parts are not fixed. This happens when the panel is, simultaneously, rotating in azimuth in, order to track the sun arrays while, it rotates in the altitude direction due to the road disturbance. For this reason, the mass moment of inertia of the panel and other parts should be determined via integration and it will be function of angle (β), figure 2 (a-b). The corresponding kinetic energy may be obtained as;

$$K.E. = \frac{1}{2}\left(\dot{\theta}_{abs.}\right)^2\left[\begin{array}{l}\frac{1}{12}Mb^2+\frac{1}{12}Ml^2\sin^2\beta\\+MR^2{}_1\cos^2\beta\end{array}\right] \quad (6)$$

θ and β are the instantaneous angular position in azimuth and altitude respectively.

The above derivation can be considered as a typical procedure and may be utilized in two different cases after specifying the instantaneous altitude angle (β). These two cases are the tracking with no disturbance in altitude, and the presence of this disturbance. In the first case, angle (β) is given as ;

$$\beta\ = \frac{\pi}{2}-\alpha-\beta_{abs.} \quad (7)$$

Where: (α) is the sun angle with respect to the vertical line, figure (2-a), which may be considered as a fixed value over short period of time.

$(\beta_{abs.})$ is the altitude angular position with reference to the sun beams, which is considered as error in the required zero angular position.

And $\dot{\beta} = -\dot{\beta}_{abs.}$ (8)

The Lagrangian is obtained to be:

$$L\left(\dot{\theta}_{abs.},\dot{\beta}_{abs.}\right)=\frac{1}{2}\left(\dot{\theta}_{abs.}\right)^2\left[\begin{array}{l}\frac{1}{12}Mb^2+\frac{1}{12}Ml^2\sin^2(\beta)+MR_1^{\,2}\cos^2(\beta)+2m_bR_b^{\,2}\cos^2(\beta)\\+2\left(\frac{1}{4}m_b r_b^{\,2}+\frac{1}{12}m_b l_b^{\,2}\right)+\left(\frac{1}{2}m_{rod}\times r_{rod}^{\,2}+\frac{1}{12}m_{rod}\times l_{rod}^{\,2}\right)\\+\left(\frac{1}{2}m_{alt-sh.}\times r_{sh.}^{\,2}+\frac{1}{12}m_{alt-sh.}\times l_{sh.}^{\,2}\right)+\left(m_{az-sh.}\times r_{sh.}^{\,2}\right)+I_e\end{array}\right]$$
$$+\frac{1}{2}\dot{\beta}_{abs.}^{\,2}\left[\begin{array}{l}\left(\frac{1}{12}M\left(l^2+t^2\right)+MR_1^{\,2}\right)+2\left[\frac{1}{2}m_b r_b^{\,2}+m_b\times R^2\right]\\+m_{alt-sh.}\times r^2{}_{sh.}+I_e\end{array}\right]$$

Having obtained the Lagrangian for the two cases, equation (2) may be applied to determine the geared motor torque, partially needed in the tracking. This is because other resistant torque is due to friction between the moving parts as well as the air drag and wind forces. Torque in azimuth and altitude are determined by the following relationships respectively;

$$T_{az} = \frac{d}{dt}\left[\frac{\partial L}{\partial\theta_{abs}}\right] = I(\beta)\times\ddot{\theta}_{abs}$$

and, $T_{alt} = \frac{d}{dt}\left[\frac{\partial L}{\partial\beta_{abs}}\right] = I_{alt}\times\ddot{\beta}_{abs}$

Where; $I(\beta)$ and I_{alt} are the total mass moment of inertia about the axis of rotation in azimuth and altitude respectively. $I(\beta)$ is evaluated by integration over the panel width and it is function of angle (β), figure (2).

4 Simulation of the Mobile Tracking System

In this work, the simulation is performed prior to the experimental tests. The mathematical model, which is developed and described earlier is used to build a block diagram using simulink. In the simulation, several cases have been examined, both for immobile sun tracking case and when the system is mobile, i.e. when it is attached to a moving vehicle.

Azimuth tracking: This case considers the azimuth tracking when the system has some sort of curvilinear motion on the ground. An (S) shaped curve is simulated and used as a disturbance to the system, figure (4). The vehicle motion is simulated to have two successive quarter circle, (turns) of a known radius (r).

The speed of the vehicle is considered to be constant at (V). This type of motion gradually produces a $(\pi/2)$ radians followed by similar but negative angle, $(-\pi/2)$ radians. The rotational speed of one part of this motion is given by $(\omega = V/r)$ rad./sec, which gives the angle as $(\theta = \omega\times t)$. It may be noticed that the function of angle (θ) is of positive ramp followed by a negative one as (ω is constant). The angular disturbance due to the vehicle motion and the correction or system rotation, relative angle, and the error, or the absolute angular position, of the panel with respect to the sun azimuth position, can be obtained.

Altitude tracking: The disturbance input function was taken to be a sinusoidal wave, figure (6). This represents an up and down topography of a wavy road. The total length and the depth (amplitude) of the road are taken (250 m) and (10 m) respectively. The speed of the vehicle is considered to be fixed at (50 km/hr). Figure (7) shows the response for this simulation.

Azimuth-Altitude tracking: In simulating this case, simultaneous disturbances for azimuth and altitude rotation as described in section (4) are applied. Figures (5) and (7) show the system responses in azimuth and altitude directions respectively. It is found that the system behavior is similar to that when any of the two road disturbances is applied to the system individually. The maximum errors in tracking sun position are (3.21°) and (2.134°) for azimuth and altitude angles respectively, and the tracking is active after

one second of the search mode which is started by $(\pi/6)$ angular error.

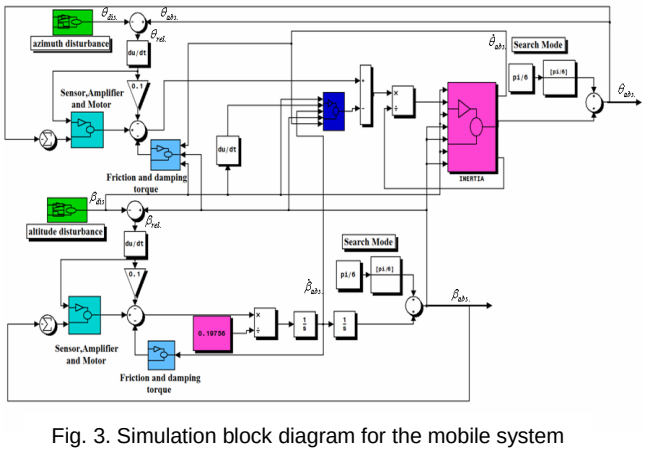

Fig. 3. Simulation block diagram for the mobile system with azimuth- altitude tracking.

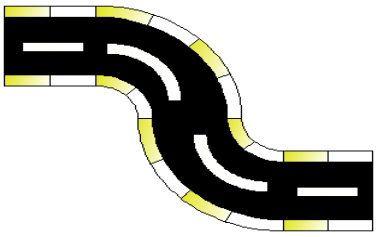

Fig. 4. Quarter-circle curvature road disturbance) for azimuth tracking

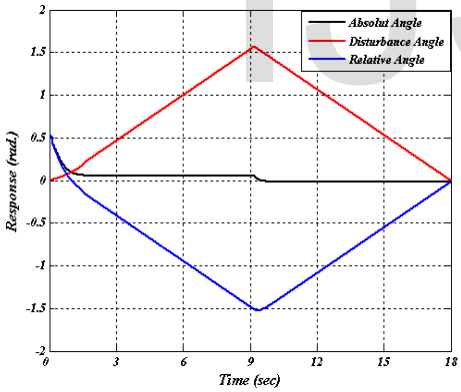

Fig. 5. The simulation response for a mobile system with azimuth-altitude tracking (azimuth angle response).

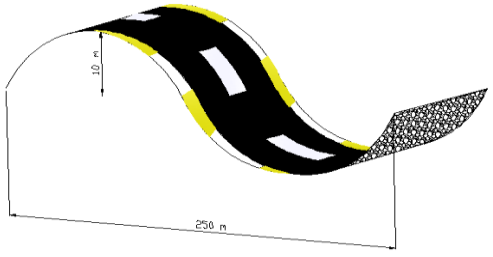

Fig. 6. Sinusoidal wave shaped road (disturbance) for altitude tracking test.

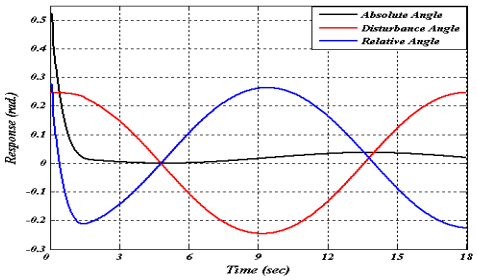

Fig. 7. The simulation response for a mobile system with azimuth-altitude tracking (altitude angle response).

5 Experimental Works

The experimental part of the work covers many separate and different tests to obtain gains and coefficients for the D.C. motors, the optical sensors, and to estimate the drag effect of air on the panel …. etc. The later was obtained for the case of fixed or immobile panel and used in the simulation, it is difficult to have a specific value for the mobile case as it is affected by many operating conditions such as air and vehicle speeds and directions. Some preliminary test was performed and compared with those of the simulation for the immobile panel, figures (8-11), i.e. without disturbance in both rotation and the system respond only to an initial error (about 60^{o} or 1 rad). The response suggest that the system is fast enough to recover this error in about one second in maximum and this reflects the search mode of figure (5) and (7). Then a series of tests were performed on the mobile system in order to understand how well the system performs in actual operation and to validate the analytical model. In this section, a description of the operation of the system is presented for different operating cases. These cases include single axis and two axes tracking. The system was fixed on the flat rear part of a small transport car. The car was driven on roads inside the university campus, where it was possible to perform some mobile one axis and two axes tracking tests. An ideal test necessitates, the avoidance of heights, high buildings, trees and bumpy roads. Avoidance of the latter was not possible because of the artificial bumps on the roads.

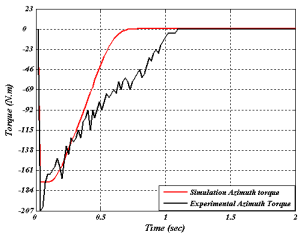

Fig. 8. motor torque for a fixed system with azimuth- altitude tracking (azimuth rotation torque).

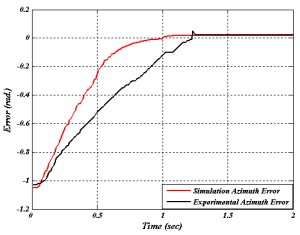

Fig. 9. The absolute angle error for a fixed system with azimuth-altitude tracking (azimuth error).

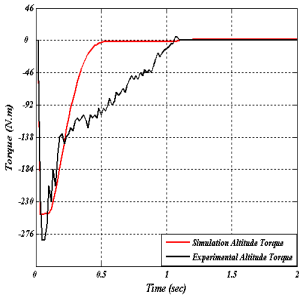

Fig. 10. motor torque for a fixed system with azimuth-altitude tracking (altitude rotation torque).

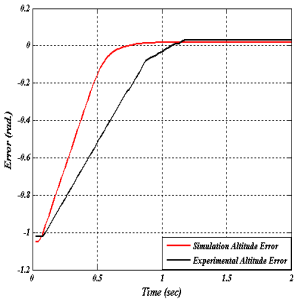

Fig. 11. The absolute angle error for a fixed system with azimuth-altitude tracking (altitude error).

Tracking Tests of the Mobile System: The sun tracking system is made mobile by fixing it on the vehicle. A car is driven on selected roads inside the university campus, so that, a U-turn, L-turn, large curve drive for azimuth and climbing a ramp-like road for altitude tests are used.

Azimuth tracking: For an azimuth tracking, a road with a U-turns is followed. The following road features has been selected as:

1. Part of the road (U-turns) is a half-circle or (π) angle of rotation).
2. The radius is to be maintained at about (8 m).
3. The speed of the vehicle is attempted to be fixed at (15 km/hr), or (4.166 m/sec).

The speed of vehicle in this type of rotation can be increased to (50 km/hr) or more, but in turn the radius of curvature has to be increased. According to the above-mentioned features, the disturbance input as function of time is of a ramp type with a rate of (0.521 rad/sec) which is fast enough to be an angular speed of rotation for a vehicle on actual roads. Data records, using the data acquisition instrument and a lab-top, is focused on the motor armature current which is proportional to the motor torque and the angular error of the tracking as an output of the sensors. Figures (12, 13) give a clear comparison between the experimental and the simulation results of the tracking for motor torque and angular error respectively.

4. Altitude tracking: In altitude tracking, the experiment is performed utilizing a road, (altitude disturbance), with the following specifications:
5. The angle of the inclination of the road was about (28°), which is equal to (0.48 rad.).
6. The vehicle speed is about (15 km/hr.).
7. In this case, the road is a ramp inclined by (0.471 rad.). This disturbance may be approximated by a step function having height of (0.471 radian). In practice, this height can not be attained suddenly, because of the length of the vehicle. Figures (14, 15) illustrate the motor torque, which is required to rotate the panel to the required position, or the correction toward the sun arrays.

Testing with two axes tracking in sequence: A road of L-shaped turn with a quarter circle turning curve of (8 m) radius, to give a (π/2) rotation are selected. The curved part of this road is followed by a (28°) inclined road while the vehicle speed is about (15 km/hr).

The behavior of the tracking system represented by the geared motor torques and angular tracking errors are shown in figures (16, 17) and (18, 19) for azimuth and altitude tracking respectively. It may be noticed that the torques jumps to a high value at the start of the tracking and converge towards almost zero at the end of the tracking period. The tracking angular errors are ended towards minimal values.

Tracking System Effectiveness: The main aim of the sun tracking system is to follow the sun beam and to keep the solar cell panel normal to the arrays of the sun, so that, more energy is absorbed, continuously, by charging the batteries. The driving D.C. motors consume part of this energy during tracking periods only.

The tracking system should be efficient if the difference between the energy produced by the photo-voltaic panel in tracking and with that without tracking is much higher than the energy consumption during tracking, i.e. the following relationship must be confirmed:

$$\varepsilon = \left(E_{PT} - E_{PF}\right) - E_C \rangle\rangle 0 \qquad (13)$$

Where: (E_{PT}) is the energy stored with tracking system in operation.

(E_{PF}) is the energy stored without tracking.

(E_C) is the energy consumed by the D.C. motor for tracking.

These energies are obtained by integrating the electric power over tracking period of time. Figure (20).

It can be noticed that the stored energy with tracking is approximately (738 J), and that without tracking, (horizontally positioned photovoltaic panel) is about (552 J), while that consumed by the driving motor is approximately (36 J) for a short period of tracking which is (1 min.) only with these turns.

Applying equation (13), the following is obtained:

$\varepsilon = 738 - (552 + 36) = 150$ Joule.

This gives a tracking effectiveness of about (27%), i.e. the collected energy by tracking system is greater than that without tracking by a factor of (1.27).

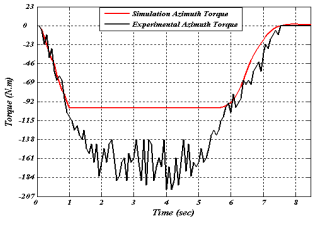

Fig. 12. Motor torque for a mobile system with azimuth tracking.

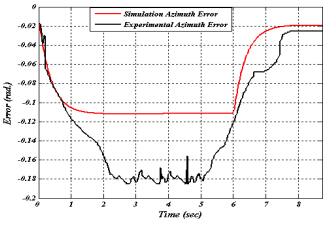

Fig. 13. The absolute angle error for a mobile system with azimuth tracking.

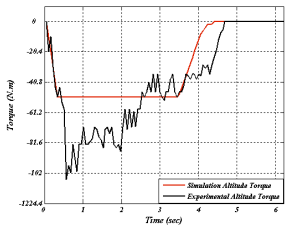

Fig. 14. Motor torque for a mobile system with altitude tracking.

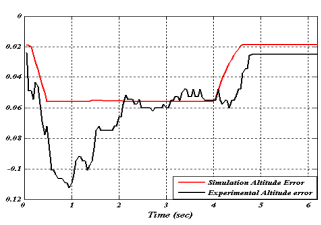

Fig. 15. The absolute angle error for a mobile system with altitude

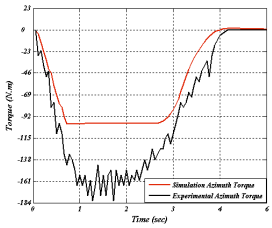

Fig. 16. Motor torque for a mobile system with azimuth-altitude tracking (azimuth rotating torque).

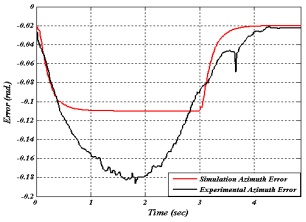

Fig.17. The absolute angle error for a mobile system with azimuth-altitude tracking (azimuth error).

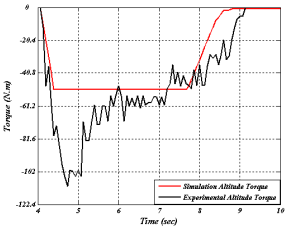

Figure (18): Motor torque for a mobile system with azimuth-altitude tracking (altitude rotating torque).

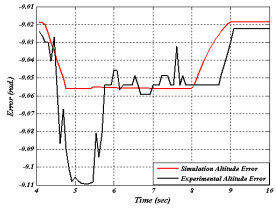

Figure (19): The absolute angle error for a mobile system with azimuth-altitude tracking (altitude error).

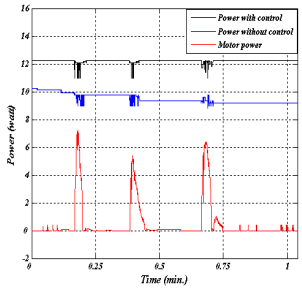

Fig. 20. The tracking effectiveness of the mobile tracking system.

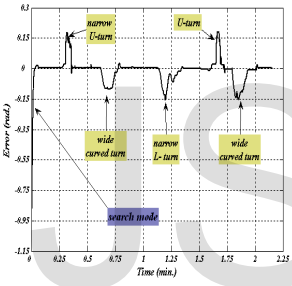

Fig. 21. The absolute error for a random vehicle drive, (azimuth tracking).

6 Discussion

In the dynamic analysis, the disturbance angles are produced by turning the vehicle and by the topography of the road, while the relative angles are produced by the rotation of the motors reduction gear which rotates in opposite direction of the disturbance, in order to correct the solar cell panel position toward the sun. The difference between the disturbance angle and the relative angle gives the absolute angle or the error with respect to the sun beams. In the experimental work, the data that have been recorded via data acquisition instrument gives the positional angular errors and the driving geared-motor's torques. These summarize the dynamical behavior of the tracking system. It can be noticed that there are some fluctuations in the torque. This fluctuation is due to road irregularities, which causes vibration of the system. In the fixed or immobile system, the torque fluctuations are much less, which is due to the gear backlash alone. This is attributed to the fact that the torque is, partially, related to the second derivative of the angular position with time. Roads that have been chosen in performing the mobile solar tracking tests are far from buildings and trees. Buildings and trees produce shadows on the photo-voltaic panel surface, which confuse the tracking process. Artificial bumps in the road are considered as an undesirable disturbance during tests, which affect the smoothness of the tracking process. The effectiveness of the mobile tracking system has been verified by performing a separate experiment as explained earlier. Inspite of driving over multiple turns in relatively short duration of tracking operation, an increase of about (27%) of the accumulated energy by the panel has been achieved. This value is not fixed, as it depends on the road profile, the sun position, the position of the panel with no tracking and the period of tracking. It is believed that the experimental results should be much better if a transparent hemispherical dome covers the panel to isolate it from wind gusting and air speed disturbance during tracking. That could lead to less power consumption of the motors, hence better effectiveness with less motor torque. An amount of steady-state error is expected as the system control is almost of proportional mode only. It is not recommended to add a derivative mode to the control as the system will be sensitive to a noisy measured signal, in addition to the unwanted disturbances affected the system. As far as the tracking performance is concerned, it is expected that angular error should be much less on normal roads on which the vehicle is driven with smooth gradual road turns and not sharp turns. However, the difference between the angle errors (Babs.) in simulation and experiment are (3^o – 4^o) in maximum, figures (13,15,17,19). In order to examine the tracking performance a test was performed for a random drive with different types of turns actuating azimuth tracking. The results were very acceptable over the (2.25 mins.) of driving period, figure (21).

7 Conclusions

Lagrangian dynamic formulation in building the mathematical model was fruitful, because the value of the mass moment of inertia for the solar cell panel is not fixed and it depends on the altitude angular position (β). A proportional control mode was found sufficient to give an overall acceptable result in the tracking as the tracking errors (absolute angles) with respect to sun beams were ended closely to zero in the simulation and experiments. The damping induced by the presence of back (emf) in the D.C. motor were greater than that due to the air drag. A gyro-moment is produced, as the system rotates in two axes. Its value is estimated to be about (0.6 N.m) in maximum, and considered as negligibly small in comparison to that provided by the geared D.C. motors. The tracking with a random drive shows that the system performs quite well and should be excellent for lengthy turns with higher speeds of the vehicle. The results of this work should be useful for cars energized by solar energy and when used on large scales arrays on the roofs of land and sea vehicles such as trains, tracks and ships, where no or small angular disturbance in the altitude is expected and for Moon or Mars Rovers when PV panels are used for energy source. The tracking in a single experiment, in after noon, gave (27%) increase in the collected energy when compared to the case of fixed panel. Figure (20).

REFERENCES

[1] Metwally, A. M., "Modeling and simulation of photovoltaic fuel hybrid system", A Dissertation in Candidacy for the Degree of Doctor in Engineering (Dr.- Ing.) university of Kassel, Germany, pp(1-5), 2005.

[2] Barkat, B., Mohammedi B., and Bendaas C., "Mechanical design of a sun tracking system with two axes for arid areas", World Renewable Energy Congress VI, Elsevier science Ltd., pp(825-831), 2000.

[3] Abu Hanieh, A., "Automatic orientation of solar photovoltaic panels", mechanical engineering dep., Birzeit university, Palestine, 2009.

[4]] Figueiredo, J. M. and Sa da Costa J. M., "Intelligent sun-tracking system for efficiency maximization of photovoltaic energy production", Technical University Lisbon, Mechatronics group, Portugal, 2008.

[5] Mamlook, R., Nijmeh S. and Abdullah S. M., "A programmable logic controller to control two axis sun tracking system", Information Technology journal 5 (6), Jordan, 1083-1087, 2006.

[6] Tegeder, T., "Development of an efficient solar powered unmanned aerial vehicle with an onboard solar tracker", M.Sc. Brigham young University, 2007.

[7] Comsit, M., and Visa I., "Design of the linkages type tracking mechanisms of the solar energy conversion systems by using Multi Body Systems Method", 12th IFToMM World Congress Besancon, pp(1-6), 2007.

[8] Partik P., et al, "Solar tracking system using Arduino", International Journal of Scientific and Engineering Research, Vol. 9, Issue 2, Feb. 2018.

[9] Tomas de J., et al, "Smart host microcontroller for optimal battery charging in a solar-powered robotic vehicle", IEEE/ASME Transaction on mechatronics, Vol. 18, No. 3, June 2013.

[10] K. Bhaskar, et al, "Solar powered vehicle under GSM network by using solar tracking and monitoring", IJEDR, Vol. 4, Issue 1, ISSN 2321-9939, 2016.

[11] Mars Exploration Rover – Wikipedia. https://en-wikipedia.org.

[12] S. W. Squyres, at al, "Overview of the apportunity Mars exploration Rover mission to Meridiani Planum: Eagle crater Purgatory Ripple", Journal of geophysical research, Vol. 111, E12S12, doi:10.1029/2006Je002771, 2006.

[13] Hammo, Kh. E., "Design and construction of a sun tracking system for a mobile solar cell panel", MSc. Thesis, Mechanical Engineering Department, University of Mosul, Iraq, 2010.

[14] Kelly, R., Santiban˜ez V., and Loria A., "Control of robot manipulator in joint space", Springer-Verlag London Limited, pp (62-65), 2005.

APPENDIX A

TABLE (A.1A): FORMULAS AND VALUES OF THE ROTATING PARTS MOMENT OF INERTIA IN ALTITUDE ROTATION:

Parts	Formula for mass moment of inertia	Values
Shaft-2-altitude	$I_{alt-sh} = m_{alt-sh} \times r_{sh}^{2}$	3.75e-5 kg.m^2
Balancing mass	$I = 2\left[\frac{1}{2} m_b r_b^{2} + m_b R^{2}\right]$	4.18e-3 kg.m^2
Solar cell panel	$I_x = \frac{1}{12} m_{pv}\left(l^2 + t^2\right) + m_{pv} R_1^{2}$	0.191 kg.m^2
equivalent moment of inertia for geared motor	$I_e = \sum_{i=1}^{i=4} I_i \left(\frac{w_i}{w_4}\right)^2$ I_i and w_i are inertia and speed of gear (i) respectively.	2.338e-3 kg.m^2

TABLE (A.1B): FORMULAS AND VALUES OF THE ROTATING PARTS MOMENT OF INERTIA IN AZIMUTH ROTATION:

parts	Moment of inertia	values
Shaft-1-azimuth	$I_{az-sh} = m_{az-sh} \times r_{sh}^{2}$	1.54e-4 kg.m^2
Shaft-2-altitude	$I_{alt-sh} = \frac{1}{2} m_{sh} r_{sh}^{2} + \frac{1}{12} m_{sh} l^{2}$	0.02 kg.m^2
Balancing mass	$2\left[\frac{1}{4} m_b r_b^{2} + \frac{1}{12} m_b l^{2} + m_b R_b^{2} \cos^2 \beta\right]$	0.207613 + $f_1(\beta)$ kg.m^2
Supporting rod for motor -1	$I_{rod} = \frac{1}{2} m_{rod} r_{rod}^{2} + \frac{1}{3} m_{rod} l^{2} + md^{2}$	0.01614 kg.m^2
equivalent moment of inertia for geared motor	$I_e = \sum_{i=1}^{i=4} I_i \left(\frac{w_i}{w_4}\right)^2$ I_i and w_i are inertia and speed of gear (i) respectively.	2.338e-3 kg.m^2
Solar cell panel	$I_z = \left[\frac{1}{12} Mb^2 + \frac{1}{12} Ml^2 \sin^2 \beta + MR^2_1 \cos^2 \beta\right]$	0.207613+ $f_2(\beta)$